Ultra-sonication enhanced green synthesis of silver nanoparticles using Barleria buxifolia leaf extract and its possible application

Vanaraj sekar (biovanam@gmail.com)
Bharathiar University

Original Research Full Papers

Keywords: Barleria buxifolia, Silver nanoparticle, Antioxidant, Antibacterial, Anticancer activity

Posted Date: February 1st, 2021

DOI: https://doi.org/10.21203/rs.3.rs-161063/v1

Abstract

A simple and eco-friendly method for the green synthesis of silver nanoparticles (AgNPs) by ultrasound-assisted strategy using *Barleria buxifolia* leaf extract as a reducing and capping agent was established in this study. The obtained AgNPs were characterized. UV-vis spectrum, Fourier transform infrared spectroscopy (FTIR), scanning and transmission electron microscopy (SEM and TEM), Energy Dispersive X-Ray Analyzer (EDX), X-ray diffraction, dynamic light scattering (DLS) analysis showed that the obtained AgNPs were mono dispersed spheres with uniform size of 80 nm. UV-vis spectroscopy, FTIR, and XRD analysis indicated that the surface of the obtained AgNPs was covered with organic molecules in plant extracts. The results of ABTS assays showed that high antioxidant activity was seen in the obtained AgNPs. Green synthesized AgNPs showed potent antibacterial and anti-biofilm activity against tested pathogens. Cytotoxicity assay showed that the obtained AgNPs were significantly cytotoxic to cancer cell line (MCF-7). In addition, the AgNPs synthesized in this paper can also photo catalytically degrade methylene blue dye under visible light. The potent bioactivity exhibited by the green synthesized silver nanoparticles leads towards the multiple use as antioxidant, antibacterial, anti-biofilm, cytotoxic as well as photo catalytic agent.

1. Introduction

In modern science, metal nanoparticles are fascinating materials with specific properties and wide application in a variety of fields, including pharmaceuticals, catalysis, food and agriculture, electronics, chemical units, cosmetics, mechanics and optics, etc. [1, 2, 3, 4, 5]. Generally metal nanomaterials synthesized by physical, mechanical, electrochemical, microwave-assisted, hydrothermal and green chemistry methods are favored [6, 7]. However, most of the physiochemical methods are extremely costly, non-degradable, and the use of toxic chemicals has contributed to multiple biological threats [8, 9, 10]. Therefore, recently the green synthesis of nanoparticles had a great attention, because of its affordable requirement like simplicity, inexpensive, biocompatibility, non-toxic, eco-friendliness and biological properties [11]. Previous papers have documented the synthesis of different metal nanomaterials via the biological method, such as plant extracts, fungi, bacteria, yeasts, and algae. [12, 13, 14, 15, 16, 17, 18, 19, 20].

As a kind of metal nanoparticles with good physical and chemical properties and biocompatibility, silver nanoparticles (AgNPs) have been widely studied. [21, 22]. The green synthesis of AgNPs through ecofriendly microbes and plant has in recent times grown to be trendy in recently. According to the reports of Gardea et al. and J. Das, P. Velusamy [23, 24], the synthesis of nanoparticles using plant extract is very simple and easy to handle compared to microbes. In these organic strategies for the synthesis of NPs, plant extracts act as reducing and capping agents. So far, Ag NPs had been efficiently and swiftly synthesized by numerous plant extract such as, *Artemisia nilagirica* [25], *Iresine herbstii* [26], *Vaccinium macrocarpon* [27], *Parthenium hysterophorous* [28], *Urticadioica Linn*. [1], *Mimusops elengi*, *Linn.* [29], *Azadirachta indica* [30], *Lonicera hypoglauca* [8], *Durio zibethinus* [7]. In addition, many scientists examined the potential properties like antioxidant, antimicrobial, antiviral, anticancer, antimalarial

properties and photo catalytic effects of green synthesized AgNPs by plant extracts [31, 32]. *Barleria buxifolia* is one of the family of acanthaceae and it have been types of secondary metabolites in the leaf, flower and root parts. The roots and leaves have been used as a traditional herbal medicine in India to deal with cough, bronchitis, inflammation and antibacterial activity against human pathogens [33, 34, 35].

With our expertise, till date there is no report on synthesis of AgNPs using *B. buxifolia*. In this direction, herein our proposed work to develop a novel approach for the biosynthesis of silver nanoparticles the usage of leaf extract of *B. buxifolia* through ultra-sonication process.

The present experimental investigation reports the green synthesis of silver nanoparticles using *B. buxifolia* leaf extract with the aid of ultra-sonication process has been mentioned. Herein we utilize *B. buxifolia* leaf extract were functions as both reducing and stabilizing agents during AgNPs synthesis. Obtained AgNPs were characterized by using UV-vis spectrum, FTIR, SEM and TEM, XRD, EDX, DLS and check its antioxidant properties using ABTS assay. Also we evaluated antibacterial, anti-biofilm and EPS reduction activity of AgNPs against pathogens such as *Escherichia coli, pseudomonas aeruginosa, Salmonella enterica, Shigella spp.* Furthermore, the synthesized AgNPs catalytic activity in the reduction of MB and their cytotoxicity toward MCF-7 breast cancer cell line has also been studied.

2. Materials And Methods

All the analytical reagents used in the study were of analytical grade and were purchased from Merck, India. Nutrient agar for bacterial culture and Mueller–Hinton broth, luria bertani broth Methylene blue, Sodium hydroxide, Methanol, Crystal violet and agar for biological were purchased from Hi-Media, Mumbai, India. MTT Assay Kit (ab211091) were also buy from Sigma Aldrich, Mumbai, India.

The MCF-7 cancer cell line was obtained from NCCS (National Centre for Cell Sciences), Pune, India. MDR Clinical pathogens were maintained in Biopharmaceutical laboratory, Bharathiar University, Coimbatore, India.

2.1. Preparation of leaf extract

B. buxifolia plant leaf were obtained from the Marudhamalai hill, Coimbatore, Tamilnadu, India. The fresh leafs were washed by distilled water, then dried and pulverized to a fine powder with the help of mortar and pestle. This powder (20 g) was the dissolved in 150 ml of methanol in a 250 ml Erlenmeyer flask, and the flask were kept in water both at 60 °C for 30 min. The solution (leaf extract) was subsequently filtered by Whatman NO.1 filter paper and hold on 4°C.

2.2. Synthesis of *B. buxifolia* leaf extract capped silver nanoparticles via Ultrasonic process

About 10 ml of crude *B. buxifolia* leaf extract was mixed with 50 mL aqueous solution of silver nitrate (0.1Mol) and the solution pH -9 were adjusted by 1M NaOH. The solution was then emulsified by subjection to high power ultrasonic vibration (40 kHz) for different time interval. Then the solution slowly

changed yellow colour to deep brown colour in ionic liquid phase, that is indicating the formation of silver nanoparticles. After the complete reduction, this solution was centrifuged at 10,000 rpm for 30 min at 4 °C. The supernatant was discarded and the pellet was re-dispersed in dd H_2O. Next, the pellet (NPs) were freeze dried and stored at vial for further use. Figure.1 indicates schematic explanation of AgNPs formation.

2.3. Characterization of AgNPs nanoparticles

UV-Vis analysis was recorded by Shimadzu UV-2500 double-beam spectrophotometer. X-ray X-ray Diffraction patterns have been recorded through a Rigaku, X-ray Diffractometer to see the phase purity of materials with diffraction angel from 20 to 80 degree. A Zeiss-EM10C Transmission Electron Microscopy (TEM) and Scanning electron microscopy (SEM) with a Cam scan MV2300 were used to study of size and morphology of nanomaterial. As well as we evaluate their elements and size via DLS. Fourier Transform Infrared (FTIR) spectra have been recorded with the help of (Thermo Scientific Nicolet 370. USA) FT-IR spectrometer in KBr pellets [36, 1].

2.4. ABTS radical scavenging activity of *B. buxifolia* leaf extract and AgNPs

ABTS solution was mixed with potassium persulphate (2.45 mM) in a ratio of 1:0.5 (v/v). The mixture was kept in dark at room temperature for 8 h. In the ABTS solution (190 µL), different concentrations (25–150 µg/mL) of standard, leaf extract and AgNPs (10 µL) solution was added. The reaction mixtures were then incubated for 6 min and the absorbance was taken at 734 nm. The change in absorbance with respective control (containing ABTS solution without antioxidants, expressed as 100% free radicals) was calculated as percentage free radical scavenging. Ascorbic acid was used as positive control [37].

$$\%\ \text{of Scavenging activity} = \frac{\text{Abs control} - \text{Abs sample}}{\text{Abs control}}\ \text{X}\ 100$$

Where A control is the absorbance of the ABTS solution and A sample is the absorbance of the test sample.

2.5. Evaluation of antibacterial activity

Antagonistic activity of the AgNPs, leaf extract biomass and amikacin have been assessed using Muller-Hinton agar well diffusion approach towards MDR clinical pathogens i.e., *P. aeruginosa, S. enterica, Shigella spp*. as per standard methods. Wells of 7 mm size are made in the Agar plates containing the bacterial lawn. The various concentration (25-100 mg/ml) of samples were filled in the wells made in the bacterial culture plates. Then the petri dishes consequently prepared were left at room temperature for ten minutes for allowing the diffusion of the samples into the agar bacterial lawn. After incubation for 24 h at

37°C, the plates had been observed. The zone of inhibition was observed and expressed in millimetres [38].

2.6. Biofilm Inhibition Assay

The ability of AgNPs with different concentrations (25-100µg/ml) to inhibit the formation of bacterial biofilms was recognized using 24 h old broth inoculums of *E. coli* and *P. aeruginosa, S. enterica, Shigella spp* using tissue culture plate method. The inoculums have been prepared using 10 ml of trypticase soy broth (TSB) with1%glucose and seeded into 1 cm^2 cover slides placed in culture plates. After 24 h, planktonic cells had been removed by way of washing using sterilized distilled water and the glass slides were stained with 0.2% crystal violet stain. Biofilms formation have been visualized by Trinocular Phase Contrast microscope (Kozo Optics) at X40magnification. After visualization, the stain was solubilized with 1ml of 70% ethanol and the stained adherent biofilm was quantified using a micro-ELISA auto reader (model R, Epoch, USA) at wavelength 570 nm [39]. The elucidation of biofilm production was finished according to the standard methodology of Stepanovic et al.2007 [40].

$$\%\ \text{of biofilm inhibition} = \frac{1 - \text{OD}_{570}\ \text{of Cells treated with AgNPs}}{\text{OD}_{570}\ \text{of non treated control}}\ \text{X}\ 100$$

2.6.1. Extraction and Quantification of EPS

Test pathogens (E. coli and *P. aeruginosa, S. enterica, Shigella spp*) are mature in liquid LB medium with presence and absence of AgNPs. The biofilms adhered to the walls of test tube were harvested at some stage in late-log-phase by vigorous shaking and centrifugation at 10,500g for 30 min at4 °C. The supernatant was filtered via 0.22 µm nitro cellulose membrane filters. Three volumes of chilled 100%ethanol was added to the filtered supernatant and incubated overnight at 4 °C to precipitate EPS. The precipitated EPS was then quantified through the technique of Dubois et al. 1956 and Vanaraj. 2017b [41, 39].

2.7. Cell viability assay

Cell viability was measured using the MTT (3- [4, 5-dimethylthiazol-2-yl]-2,5diphenyltetrazolium bromide) dye-reduction assay to determine the cytotoxic impact of the DOX and AgNPs at various concentrations. Briefly, cells were plated onto 96-well flat-bottom culture plates with various concentrations of DOX and AgNPs (25, 50, 75, 100 µg/ml). All cultures were incubated for 48 hours at 37°C in a humidified incubator. After 48 hours of incubation (37°C, 5% CO2 in a humid atmosphere), 10 µL of MTT (5 mg/mL in PBS) was added to every well, and the plate was incubated for a further 4 hours at 37°C. The resulting Formosan was dissolved in 100 µL of dimethyl sulfoxide with gentle shaking at 37°C, and absorbance was measured at 595 nm with an enzyme linked immune sorbent assay reader (Spectra Max; Molecular Devices, Sunnyvale, CA, USA). The results were given as the means of three independent experiments.

Concentrations of DOX and AgNPs showing a 50% reduction in cell viability (i.e., half-maximal inhibitory concentration [IC50] values) were then calculated. Cell viability expressed as follows [42]:

$$\%\ \text{OF Cell viability} = \frac{\text{Experimental OD}_{595}}{\text{Control OD}_{595}}\ \text{X}\ 100$$

2.7.1. Morphological assays

The MCF-7 cells that were grown on coverslips (1×105 cells/cover slip) were incubated with AgNPs and DOX with different concentrations (0, IC_{50} and 100 µg/ml), and they were fixed in an ethanol/acetic acid solution (3:1, v/v). The cover slips were gently mounted on glass slides for morphometric analysis. Three monolayers per experimental group were photo micro graphed. The morphological changes of the MCF-7 cells were analysed using Trinocular Phase Contrast microscope (Kozo Optics) at X40magnification.

2.8. Photocatalytic degradation of dye

Photocatalytic things to do of the green synthesized AgNPs estimated from the degradation of methylene blue (MB) under the sun light irradiation for distinctive time interval. 1mg of methylene blue dye used to be dissolved in 100mL of double distilled water used as inventory solution. About 20 mg of green synthesized AgNPs was dispensed to 50mL of methylene blue dye solution. A control was also maintained without addition of AgNPs. Before exposing to irradiation, the reaction suspension was nicely blended by means of being magnetically stirred for 30min to certainly make the equilibrium of the working solution. Then, the dispersion used to be put under the sunlight and it monitored from morning to sunset. At particular time intervals, aliquots of 5mL suspension had been taken and filtered to evaluate the photocatalytic degradation of dye via UV spec two at 200-700nm [43]

2.9. Statistical analysis

Green synthesized AgNPs were assayed for antibiofilm, antimicrobial, anticancer and photo-catalytic activity. All the experiment were run in triplicates and data were reported as mean ± standard deviation and the data were analysed by one-way ANOVA Tukey's HSD analysis of variance, with a P-value of 0.05 being significant, using the (IBM SPSS statistics 20) statistical software package.

3. Results And Discussion

3.1. Ultra-sonic intensified synthesis and characterization of AgNPs using *B. buxifolia* leaf extract:

The present study integrates ultra-sound intensified green approach to produce silver nanoparticles using *B. buxifolia* leaf extract as both reducing and stabilizing agent. In a typical greener procedure, an appropriate amount (10ml) of leaf extract was dissolved in 50 ml of silver nitrate solution. Then, an ultrasonic probe was immersed into the mixture solution for various time interval (0- 240 min), whereas

exposing to ultrasound waves on Ag^+ ions containing leaf extract changed from light yellow to darkish brown colour, which suggest the formation of AgNPs via bioreduction process (Ag^+ converted to Ag^0, during the addition of polyphenols). The Ag^+ ions without leaf extract did not show any colour changes even exposing to ultra-sonication for 240min. From Fig. 1a. the UV–Vis results, it is found that green synthesised AgNPs are mono dispersed in nature and broad surface plasmon resonance(SPR) peak was also observed at 435 nm with high intensity for the increasing time, which indicates the formation of AgNPs and their stability. Earlier reports recommended that an SPR shift situated from 410 to 450 nm has been detected for AgNPs, which also attributed to spherical in nature [1, 44] and their size range in 2nm-100nm [45]. Also our results consist with [2, 46, 47] that synthesized silver nanoparticles using plant extract; they obtained the maximum absorption shift at 440, 430, 450 nm and they cited the band came about due to the surface plasmon resonance of AgNPs. According to these results we suggest, that the process of ultra-sonication makes the silver nanoparticles intrinsically capping with plant molecules and it produced size controlled spherical shape like non-aggregated mono dispersed particles, as well as these techniques gives to a treasured contribution in nano-biotechnology.

The phase purity and crystalline nature of synthesised AgNPs is studied with the aid of X-ray diffraction analysis as given in Fig. 1b. Herein, we observed the crystalline peaks at 2Θ= 38.21°, 44.38, 64.56° and 77.39°, these peaks are attributed to the (111), (200), (220) and (311) crystallographic planes. Those peaks are consistent with the JCPDS card No 65-2871of the AgNPs. Also our results strongly agreement with previous reports, that the sharp diffraction peaks with negligible noise verify the high quality of crystallinity that attributed to face-centered cubic (fcc) spinel structure of AgNPs [48, 49]. In this manner, the normal grain size of the AgNPs was computed from the solid reflection peak by (111) arrangement utilizing Scherer formula.

$$Dc = \frac{K\lambda}{\beta Cos\theta}$$

From this equation, the common size of AgNPs became approximately in 80 nm. In addition, the X-ray diffraction results clearly shows that the silver nanoparticles formed by the reduction of Ag+ ions by the *B. buxifolia* leaf extract are crystalline in nature. Further, unassigned peaks at 2θ = 32.35°, 46.31°, 54.56°, and 57.58° denoted by (*) that's indicating the presence of plant extract (capping agent) with the AgNPs as summarized in Figure 2b, the similar results were reported by Awwad et al. 2013 [50].

The nano structures of the green synthesized AgNPs by *B. buxifolia* leaf extract have been studied through scanning electron microscopy (SEM) and transmission electron microscopy analysis which illustrated that AgNPs are mostly spherical in shape without aggregation of nanoparticles. A typical SEM and TEM image showing the size and morphology of the nanoparticles is given in Fig. 1c and 1d. The presence of chemical elements was analysed using an EDS study of 0 to 10. keV and showed the characteristic peaks for pure metal silver and the presence of 52.40 % silver was a clear indicator of the

AgNP synthesis, which is shown in Fig. 1g. The average size of the colloidal AgNPs was measured by dynamic light scattering (DLS) detector. Fig. 1e shows that the average particles size was found to be 80 nm in diameter with poly-dispersed (pdi-0.243) in nature.

FTIR measurements were carried out in direction to pick out the presence of various functional group in green synthesized AgNPs using *B. buxifolia*. Fig. 1f shows absorption bands at 1348.20, 1382.96, 1593.20, 2360.67, 2725.42, 2810.28, 2926.06 and 3410.15 cm^{-1} specifying the presence of plant extract in AgNPs. The broad shift present at 3410.15 cm^{-1} in the spectra agrees to O-H stretching vibration showing the presence of phenols and alcohol. In addition, the band at 1593.20 cm^{-1} corresponds to amide C=O stretching and some other peaks located at 2926.06, 1348.20, and 1382.96cm^{-1} respectively, which are agree to C-H stretch (alkanes); C=C stretch (aromatic ring); C-H (aromatics) suggesting, that presence of phytochemicals. FT-IR results revealed that alcoholic, phenols, aromatic and amine groups may act as a capping and stabilizing agent of Ag+ ions to AgNPs [29, 51, 52].

3.2. ABTS radical scavenging activity

Antioxidants are molecules that prevent cell damage by reacting with the free radicals and have proved critical in infection management of bacterial, fungal and viral disease as well as Cancer, HIV and inflammatory diseases in human. ABTS radical inhibition of leaf extract biomass and AgNPs using different concentration compared to standard (ascorbic acid) which was shown in (Fig 2) respectively. Although ascorbic acid used as a positive control in this manner, it has been showed the highest antiradical action. Thus, AgNPs show tremendous free radical activity in significantly with expanding concentration in the range of 25–150 µg/ml when compared with standard and leaf extract biomass. The greatest free radical-scavenger activity was represented the green synthesised AgNPs, standard and leaf extract biomass estimations of 95.65 ±1.6%, 89.57±3.1 % and 70.85±1.5 % separately. Our study strongly agreement with earlier studies, that the ability of AgNPs synthesized using leaf extracts prepared from *E. scaber* and *P. granatum* as good scavengers of free radicals [53, 54]

3.3. Analysis of antibacterial activity of green synthesized Ag-NPs

The antibacterial property of green synthesized AgNPs, leaf extract biomass and amikacin was tested against MDR strains such as *E. coli* and *P. aeruginosa, S. enterica, Shigella spp*. This was quantified by the agar well diffusion assay, wherein the zone of inhibition acquired by plating the organisms on a Muller-Hinton agar plate and performing the well diffusion test for various concentrations (25, 50and 100 µg/ml) for 24hr. The AgNPs, leaf extract biomass and amikacin are exhibited significant (ANOVA, $P<0.05$) antibacterial activity against tested pathogens at dose dependant manner and the results were summarized in Table 1. Overall, our results indicate that Silver nanoparticles have better antibacterial property than the commercial antibiotic and leaf extracts biomass. In addition, here we observed highest zone of inhibition present at maximum inhibitory concentration of AgNPs (100µg/ml) on *S.enterica* (25.40±0.83) followed by *E. coli* (21.6±1.10), *Shigella spp* (19.4±0.97) and *P. aeruginosa* (18.6±1.25). Furthermore, the minimum inhibitory concentration (25µg/ml) also shows better activity which are

displayed in Table 1. Other than that, silver nanoparticles synthesised with aqueous extract of *Rivina humilis* leaves and *Pistacia atlantica* leaf extract were also strongly inhibited at low concentrations in the growth of all tested bacteria [55, 56]. Also our results strongly committed with old reports, that the AgNPs exhibited more antibacterial activity than other nanoparticles because of their physical and chemical properties [57, 58]. As well as some studies reports, that green synthesized AgNPs initiate continuous oxidative stress on bacterial cell wall, it may leads to bacterial cell death [59,60]. Therefore, our findings suggest, that the green synthesized AgNPs from *B. buxifolia* and its antibacterial properties may be useful to food preservation technique, biomedical, cosmetic and agriculture field.

3.4. Anti-biofilm and EPS inhibition activity of Ag-NPs

Biofilms inhibition of *E. coli* and *P. aeruginosa, S. enterica, Shigella spp* with different concentration of AgNPs were imaged by light microscopy. The samples were stained with crystal violet to differentiate between control (without AgNPs) and treated biofilm (with AgNPs). Violet colour indicates the presence of bacterial cells with compromised membranes, which is shown in Fig. 3. From this results here we observed, that biofilm inhibition and biofilm disruption or cell dispersion occurred at dose dependant manner. The AgNPs showed effective anti-biofilm activity towards the tested biofilm producers. From Fig. 4 (a, b, c, d), it was observed that all the concentrations of AgNPs showed good anti-biofilm activity, even at minimal concentration of 25µg/ml. Current results revealed the anti-biofilm activity of AgNPs on *Salmonella* was significantly higher than other tested bacteria ($p < 0.05$). In this case, the amount of biofilm formation was sharply decreased by increasing concentration (BIC) of AgNPs at 100µg/ml (96.1 ±1.37% inhibition) and (90.3 ± 1.1% inhibition) (86.7 ± 1.5% inhibition) (76.3 ± 1.2% inhibition) for *E. coli, S. enterica, P. aeruginosa* and *Shigella spp*. The toxicity of green synthesized silver nanoparticles against bacterial pathogen, may be due to the small size of nanoparticles, which penetrate into the cell wall, where they interfere with moulting and change the physiological processes [39].

The synthesized AgNPs were able to reduce the exo poly substances (EPS) of *E. coli* and *P. aeruginosa, S. enterica, Shigella spp*. The concentration of the AgNPs used to assess the EPS inhibition ranged from 25 µg - 100 µg /ml. From Fig. 4 (a1, b1, c1, d1), it was observed that all the concentrations of AgNPs showed significant reduction of EPS production. The test AgNPs at 100 µg/ml exhibited 98.4±1.4%, 95.3±1.0%, 91.7±1.4 and 84.6% decrease in EPS production of *E. coli, S. enterica, P. aeruginosa* and *Shigella spp*. This result also indicates the disruption of biofilm architecture. Our results correlated with Park et al. 2013 [61] reported, that silver nanoparticles had more toxic against bacterial cells and their extracellular substance.

3.5. Cytotoxicity/cell viability of AgNPs in MCF-7 cells

Breast cancer cell line (MCF-7) were exposed to AgNPs and Doxorubicin (DOX) at the concentrations of 0 µg/mL, 20 µg/mL, 40 µg/mL, 60 µg/mL and 100 µg/mL for 48 hours, and cytotoxicity was determined by MTT assay which are summarized in Fig 5 a. This results revealed, that % of cell viability was sharply decreased by increase in AgNPs and Dox concentration. While in case of AgNPs, the 50 % inhibition in

breast cancer cell line was seen at 48 µg/mL for MCF-7 cell line. In addition, the IC_{50} values for Dox were 37 µg/mL for MCF-7 cell line respectively. From these results, it was understood that the green synthesized AgNPs were less toxic, as well as similar anticancer activity compared with conventional drug. This results are strictly dealing with the earlier investigations [62]. In cancer cells, AgNPs cause reactive oxygen species to damage the cellular components that lead to cell death [63].

In comparison with untreated cells, morphological changes were observed in AgNPs (IC_{50} and 100 g/mL) and DOX (IC_{50} and 100 g/mL) treated MCF-7 cells. Cytoplasmic condensation, cell shrinkage, which is summarised in this study Fig 5b, was the most identifiable morphological changes of AgNPs and DOX-treated cells seen in this study. In agreement with our findings, recent research pointed out that AgNPs may attached to the membrane of cancer cells due to their electrostatic interaction and cause a process of pore formation on cell surface, cell shrinkage, membrane blabbing and deactivation of DNA and Mitochondria, that may ultimately lead to the cell death [64, 65].

3.6. Photocatalytic activity of AgNPs

Methylene Blue is a highly toxic, synthetic dye that can essentially be used in the pharmaceutical, textile and dyeing industries. The effect of this poisonous compound can result in the destruction of equilibrium in water bodies and living systems. [66, 67]. In this direction, current study examined photocataytic activity of AgNPs against MB. The experiment resulted in the execution of the following conditions: 50 ml of MB with 20 mg of AgNPs nanoparticle and this reaction mixture was kept in sunlight for various time intervals. During this reaction, the MB was photo degraded in the stepwise manner with the colour of the solution changing from a preliminary deep blue to almost transparent. The absorbance intensity decreases gradually with increasing of the contact times, which shows the photocatalytic degradation that was proven in Fig 6a. Methylene blue does not degrade under the irradiation of sun light without the use of AgNPs. Fig. 6b shows the amounts of MB degraded for various concentrations of AgNPs (2.5mg, 5mg, 10mg, 15mg, 20mg) and their % removals are 25, 56, 77, 82 and 83% respectively. In line with our results, it could be concluded that the green synthesized AgNPs had a dose dependent and time dependent manner degradation of MB. Our results strongly agree with previous reports that the green synthesized AgNPs have effective photocatalytic properties [15].

4. Conclusion

In conclusion, we have developed a simple and ultra-sonication intensified green approach closer the enhancement of a new technique for the synthesis of silver nanoparticles (Ag NPs). The formation of AgNPs starts quickly after the addition of $AgNO_3$ with *B. buxifolia* leaf extract with the aide of ultrasonic vibration. According to our knowledge, it is very first time for synthesis of AgNPs using *B. buxifolia* via ultra-sonication process. The AgNPs have been accurately characterized by UV, XRD, SEM, TEM, DLS and FTIR analysis. Characterization fact showed that the AgNPs had been crystalline in nature and physical identification expose the spherical shape with size range at 80 nm. The green synthesized AgNPs exhibit strong antioxidant properties and enhanced antibacterial, anti-biofilm and EPS inhibition activity against

MDR strains such as *E. coli, S. enterica, P. aeruginosa* and *Shigella spp*. Additionally good anticancer impact towards breast cancer cell lines (MCF-7) and less toxic compared to commercial drug (Doxorubicin). As well as the MB is successfully degraded by AgNPs act as photocatalyst under the sun light condition. From our studies, we stated that a simple, unhazardous, cost-less, eco-friendliness is some promising points of the ultrasonic aided green process, and this method reduces the time to make the nano crystals without agglomeration. Therefore, we believe that our findings make a valuable contribution to different fields such as food preservation, pharmaceutical, agricultural and textile industries.

Declarations

Acknowledgement

This research project was financially supported by National Natural Science Foundation of China (grant no.31972172), Natural Science Foundation of Jiangsu Province (grant no. BK20170070), Jiangsu Province Foundation for talents of six key industries (grant no. NY-013 and JNHB-131) and Jiangsu University Research Fund (grant no. 11JDG050).

Declarations of interest: None

References

1. Jyoti, K., Baunthiyal, M., & Singh, A. J RADIAT RES APPL SC, 9 (2016) 217-227.
2. Rahman, A.U., Khan, A.U., Yuan, Q., Wei, Y., Ahmad, A., Ullah, S., Khan, Z.U.H., Shams, S., Tariq, M. and Ahmad, W. J. Photochem. Photobiol. B, Biol, 193 (2019) 31-38.
3. Yang, B., Yang, Z., Wang, R., & Feng, Z. J MATER CHEM A, 2 (2014) 785-791.
4. Bastus, N. G., Merkoci, F., Piella, J., &Puntes, V. Chem. Mater, 26 (2014) 2836-2846.
5. Boca, S. C., Potara, M., Gabudean, A. M., Juhem, A., Baldeck, P. L., &Astilean, S. Cancer Lett, 311 (2011)131-140.
6. Zhang, B. Gokce, S. Barci kowski. Chem. Rev, 117 (2017) 3990–4103.
7. Sengan, M., Veeramuthu, D., &Veerappan, A. Mater. Res. Bull, 100 (2018) 386-393.
8. Jang, S. J., Yang, I. J., Tettey, C. O., Kim, K. M., & Shin, H. M. Mater. Sci. Eng. C, 68 (2016) 430-435.
9. Cheng, J.W. Betts, S.M. Kelly, J. Schaller, T. Heinze. Green Chem, 15 (2013) 989–998.
10. He, J., Kunitake, T., &Nakao, A. Chem Mater, 15 (2003)4401-4406.
11. Chandran, S. P., Chaudhary, M., Pasricha, R., Ahmed, A., & Sastry, M. Biotechnol. Prog, 22 (2006) 577-583.
12. Mohapatra, B., Kuriakose, S., & Mohapatra, S. J ALLOY COMPD, 637 (2015) 119-126.
13. Yokoyama, K., &Welchons, D. R. Nanotechnology, 18 (2007) 105-101.
14. Veisi, H., Hemmati, S., Shirvani, H., Veisi, H. Appl. Organomet, 30 (2016a)387-391.

15. Khan, S. A., Bello, B. A., Khan, J. A., Anwar, Y., Mirza, M. B., Qadri, F., & Khan, S. B. J. Photochem. Photobiol. B, Biol, 182 (2018) 62-70.
16. Sinha, I. Pan, P. Chanda, S.K. Sen. J. Appl. Biosci, 19 (2009) 1113–1130.
17. Thakkar, K. N., Mhatre, S. S., & Parikh, R. Y. Nanomedicine, 6 (2010) 257-262.
18. Rao, K. J., & Paria, S. Mater. Res. Bull, 48 (2013) 628-634.
19. Dubey, S. P., Lahtinen, M., & Sillanpaa, M. Process Biochem, 45 (2010) 1065-1071.
20. Kasthuri, J., Kathiravan, K., & Rajendiran, N. J Nanopart Res, 11 (2009) 1075-1085.
21. Shaham, G., Veisi, H., & Hekmati, M. Appl. Organomet, 31(2017)37-35.
22. Azizi, Z., Pourseyedi, S., Khatami, M., Mohammadi, H. J CLUST SCI, 27 (2016) 1613-1628.
23. Gardea-Torresdey, J. L., Gomez, E., Peralta-Videa, J. R., Parsons, J. G., Troiani, H., & Jose-Yacaman, M. Langmuir, 19 (2003) 1357-1361.
24. Das, J., &Velusamy, P. Nano Biomed. Eng, 5 (2013) 34-38.
25. Vijayakumar, M., Priya, K., Nancy, F. T., Noorlidah, A., & Ahmed, A. B. A. Ind Crops Prod, 41 (2013) 235-240.
26. Dipankar, C., &Murugan, S. Colloids Surf. B, 98 (2012) 112-119.
27. Khodadadi, B., Bordbar, M., Yeganeh-Faal, A., &Nasrollahzadeh, M. J ALLOY COMPD, 719 (2017) 82-88.
28. Adur, A. J., Nandini, N., Mayachar, K. S., Ramya, R., & Srinatha, N. J. Photochem. Photobiol. B, Biol, 183 (2018) 30-34.
29. Prakash, P., Gnanaprakasam, P., Emmanuel, R., Arokiyaraj, S., & Saravanan, M. Colloids Surf. B, 108 (2013) 255-259.
30. Ahmed, S., Saifullah, Ahmad, M., Swami, B. L., & Ikram, S. J RADIAT RES APPL SC, 9 (2016) 1-7.
31. Murugan, K., Venus, J. S. E., Panneerselvam, C., Bedini, S., Conti, B., Nicoletti, M., Santose Kumar. Environ. Sci. Pollut. Res, 22 (2015) 17053-17064.
32. Chung, I. M., Park, I., Seung-Hyun, K., Thiruvengadam, M., & Rajakumar, G. Nanoscale Res. Lett, 11 (2016) 40.
33. Chander, P. A., Sri, H. Y., Sravanthi, N. B., & Susmitha, U. V. Asian Pac. J. Trop. Dis., 4 (2014) S233-S235.
34. Chetty, K. M., Sivaji, K., & Rao, K. T., Flowering Plants of Chittoor District, Andhra Pradesh, India. Student Offset Printers, Tirupati India, (2008) 34-35.
35. Tamil Selvi, S., Jamuna, S., Thekan, S., & Paulsamy, S. JAHM, 3 (2017) 63-77.
36. Roni, M., Murugan, K., Panneerselvam, C., Subramaniam, J., & Hwang, J. S. J Parasitol Res, 112 (2013) 981-990.
37. Al-Shmgani, H. S., Mohammed, W. H., Sulaiman, G. M., & Saadoon, A. H. Artif Cells Nanomed Biotechnol, 45-6 (2017), 1234-1240.
38. Vanaraj, S., Jabastin, J., Sathiskumar, S., &Preethi, K. J CLUST SCI, 28 (2017 a) 227-244.

39. Vanaraj, S., Keerthana, B. B., &Preethi, K. J Inorg Organomet Polym Mater, 27 (2017 b)1412-1422.
40. Stepanovic, S., Vukovic, D., Hola, V., Bonaventura, G. D., Djukic, S., Cirkovic, I., & Ruzicka, F. APMIS, 115 (2007) 891-899.
41. Dubois, M., Gilles, K. A., Hamilton, J. K., Rebers, P. T., & Smith, F. Anal. Chem, 28 (1956) 350-356.
42. Vivek, R., Thangam, R., Muthuchelian, K., Gunasekaran, P., Kaveri, K., &Kannan, S. Process Biochem, 47 (2012) 2405-2410.
43. Anbuvannan, M., Ramesh, M., Viruthagiri, G., Shanmugam, N., & Kannadasan, N. Mater Sci Semicond Process, 39 (2015) 621-628.
44. Zaheer, Z., & Rafiuddin. Colloids Surf. B, 90 (2012) 48-52.
45. Pradhan, N., Pal, A., & Pal, T. Colloids Surf., 196 (2002) 247-257.
46. Rao, N. H., Lakshmidevi, N., Pammi, S. V. N., Kollu, P., Ganapaty, S., & Lakshmi, P. Mater. Sci. Eng. C, 62 (2016) 553-557.
47. Balwe, S. G., Shinde, V. V., Rokade, A. A., Park, S. S., & Jeong, Y. T. Catal. Commun, 99 (2017) 121-126.
48. Vincent, S., Kovendan, K., Chandramohan, B., Kamalakannan, S., Kumar, P. M., Vasugi, C.& Benelli, G. J CLUST SCI, (2016)1-22.
49. Markowska, K., Grudniak, A. M., & Wolska, K. I. Acta Biochim., 60 (2013).
50. Awwad, A. M., Salem, N. M., &Abdeen, A. O. Int. J. Ind. Chem., 4 (2013) 29.
51. Baghbani-Arani, F., Movagharnia, R., Sharifian, A., Salehi, S., & Shandiz, S. A. S. J. Photochem. Photobiol. B, Biol, 173 (2017) 640-649.
52. Balaji, D. S., Basavaraja, S., Deshpande, R., Mahesh, D. B., Prabhakar, B. K., & Venkataraman, A. Colloids Surf. B, 68 (2009) 88-92.
53. Kharat, S. N., & Mendhulkar, V. D. Mater. Sci. Eng. C, 62 (2016) 719-724.
54. Saratale, R. G., Shin, H. S., Kumar, G., Benelli, G., Kim, D. S., & Saratale, G. D. Artif Cells Nanomed Biotechnol, 46-1 (2018) 211-222.
55. Hamelian, M.M. Zangeneh, A. Shahmohammadi, K. Varmira, H. Veisi. Appl Organometal. Chem 33 (2019) e5278.
56. Raghava, S., Mbae, K. M., & Umesha, S. Saudi Journal of Biological Sciences, 28-1 (2020) 495-503.
57. Dipankar, C., &Murugan, S. Colloids Surf. B, 98 (2012) 112-119.
58. Ghosh, S., Patil, S., Ahire, M., Kitture, R., Kale, S., Pardesi, K., Cameotra, S.S., Bellare, J., Dhavale, D.D., Jabgunde, A. and Chopade, B.A. INT J NANOMED, 7 (2012) 483.
59. Dakhil, A. S. J. King Saud Univ. Sci, 29 (2017) 462-467.
60. Hemlata, Meena, P. R., Singh, A. P., & Tejavath, K. K. ACS omega, 5-10 (2020) 5520-5528.
61. Park, Hee-Jin, HeeYeon Kim, Seoeun Cha, Chang Hoon Ahn, Jinkyu Roh, Soomin Park, Sujin Kim. Chemosphere, 92 (2013) 524-528.
62. Kummara, S., Patil, M. B., & Uriah, T. Biomed Pharmaco Ther, 84 (2016) 10-21.
63. Jacob, S. J. P., Finub, J. S., & Narayanan, A. Colloids Surf. B, 91(2012) 212-214.

64. P. Kannan, R. Ramesh, P. Subramanian, R. Thirumurugan. Mater. Res. Bull, 49 (2014) 494–502.
65. Carlson, C., Hussain, S. M., Schrand, A. M., K. Braydich-Stolle, L., Hess, K. L., Jones, R. L., &Schlager, J. J. J PHYS CHEM B, 112 (2008) 13608-13619.
66. Baeissa, E. S. Front nosi noteh, 2 (2016) 1-5.
67. Kumar, M. S., Supraja, N., & David, E. J. Bioequivalence Bioavailab, 4 (2019) 1-7.

Tables

Table 1: Antimicrobial activity of green synthesized AgNPs, *B. buxifolia* leaf extract biomass and Amikacin.

Sample	Bacteria	Zone of inhibition (mm)		
		Concentration of samples		
		25 µg/mL	50 µg/mL	100 µg/mL
B. buxifolia leaf extract biomass	*E-coli*	2.20±0.45^{c}	5.25±0.32^{b}	11.2±0.25 ^{a}
	P. aeruginosa	0.0 ± 0.0^{c}	3.29± 0.80 ^{b}	8.00±1.40 ^{a}
	Shigella spp	3.22±0.43^{c}	7.5±0.30^{b}	13.2± 0.88^{a}
	Solmonilla	5.10± 1.24^{c}	11.34± 1.44^{b}	15.36± 0.72^{a}
Green synthesized AgNPs	*E-coli*	6.6±0.60^{c}	15.6±0.73^{b}	21.6±1.10 ^{a}
	P. aeruginosa	3.7 ± 0.78^{c}	11.5± 0.75 ^{b}	18.6±1.25 ^{a}
	Shigella spp	5.36±0.86^{c}	13.6±1.26^{b}	19.4± 0.97^{a}
	Solmonilla	8.74± 0.62^{c}	18.53± 1.02^{b}	25.40± 0.83^{a}
Amikacin (commercial antibiotic)	*E-coli*	4.0±0.95^{c}	9.34±0.50^{b}	16.43±0.25 ^{a}
	P. aeruginosa	2.4 ± 0.7^{c}	6.88± 0.42 ^{b}	15.20±0.79 ^{a}
	Shigella spp	4.86±0.20^{c}	10.0±0.55^{b}	17.30± 1.40^{a}
	Solmonilla	6.36± 0.98^{c}	14.0± 1.10^{b}	19.0± 0.90^{a}

Values mean ± SD indicates the replicates of three experiments.

* Mean values within the column followed by the same ANOVA letter in superscript are significantly different at P < 0.05 level.

Figures

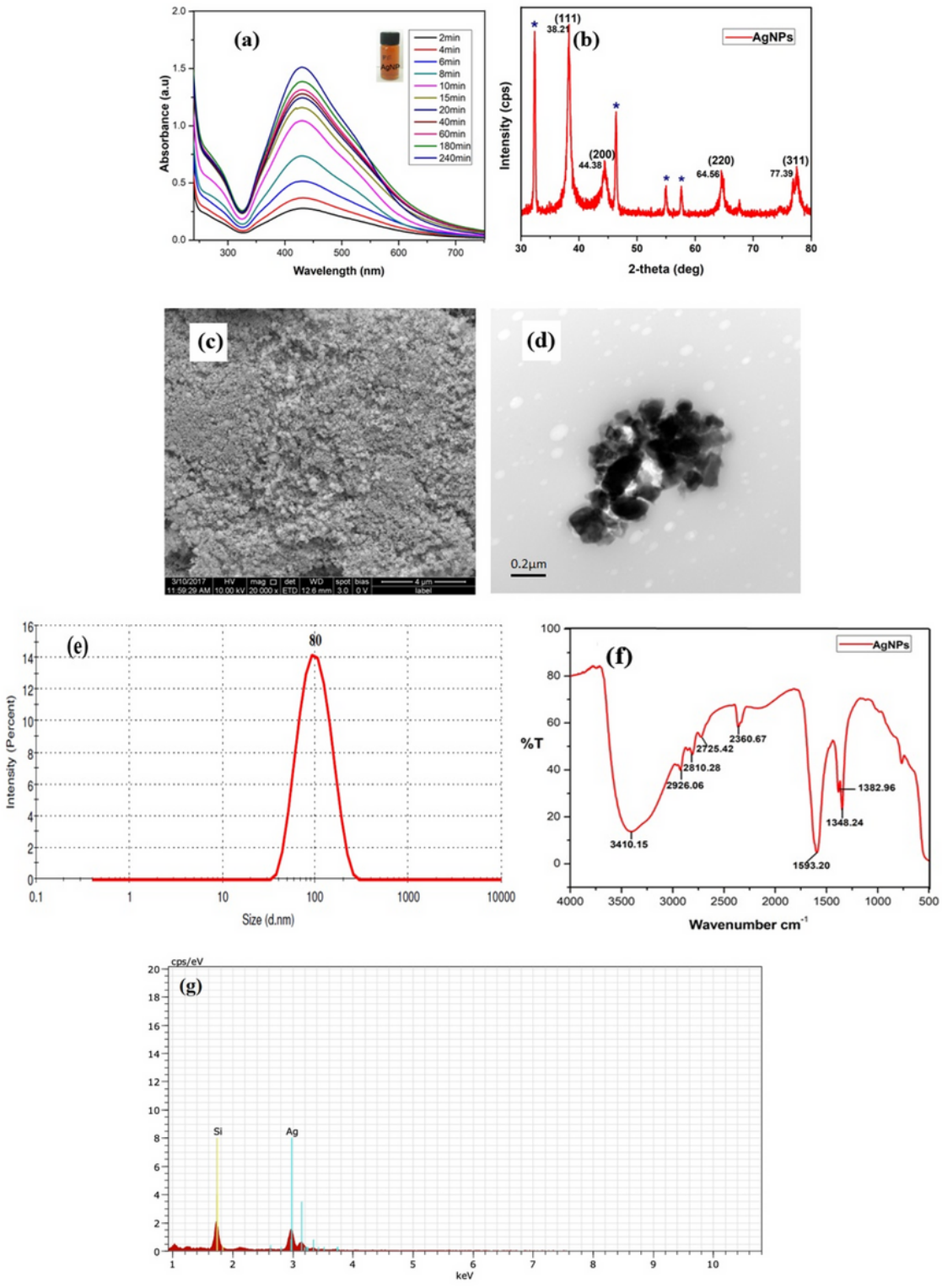

Figure 1

Morphological identification and chemical properties of green synthesized silver nanoparticles (a) UV-Vis spectra of AgNPs prepared using B. buxifolia methanolic leaf extract with various times and (b) XRD pattern of green synthesized AgNPs, (c) Scanning Electron Microscopy (SEM) image of synthesized

AgNPs, (d) Transmission Electron Microscope (TEM) image of AgNPs and (e) Dynamic light scattering (DLS) results of AgNPs, (f) FT-IR spectrum of prepared AgNPs.

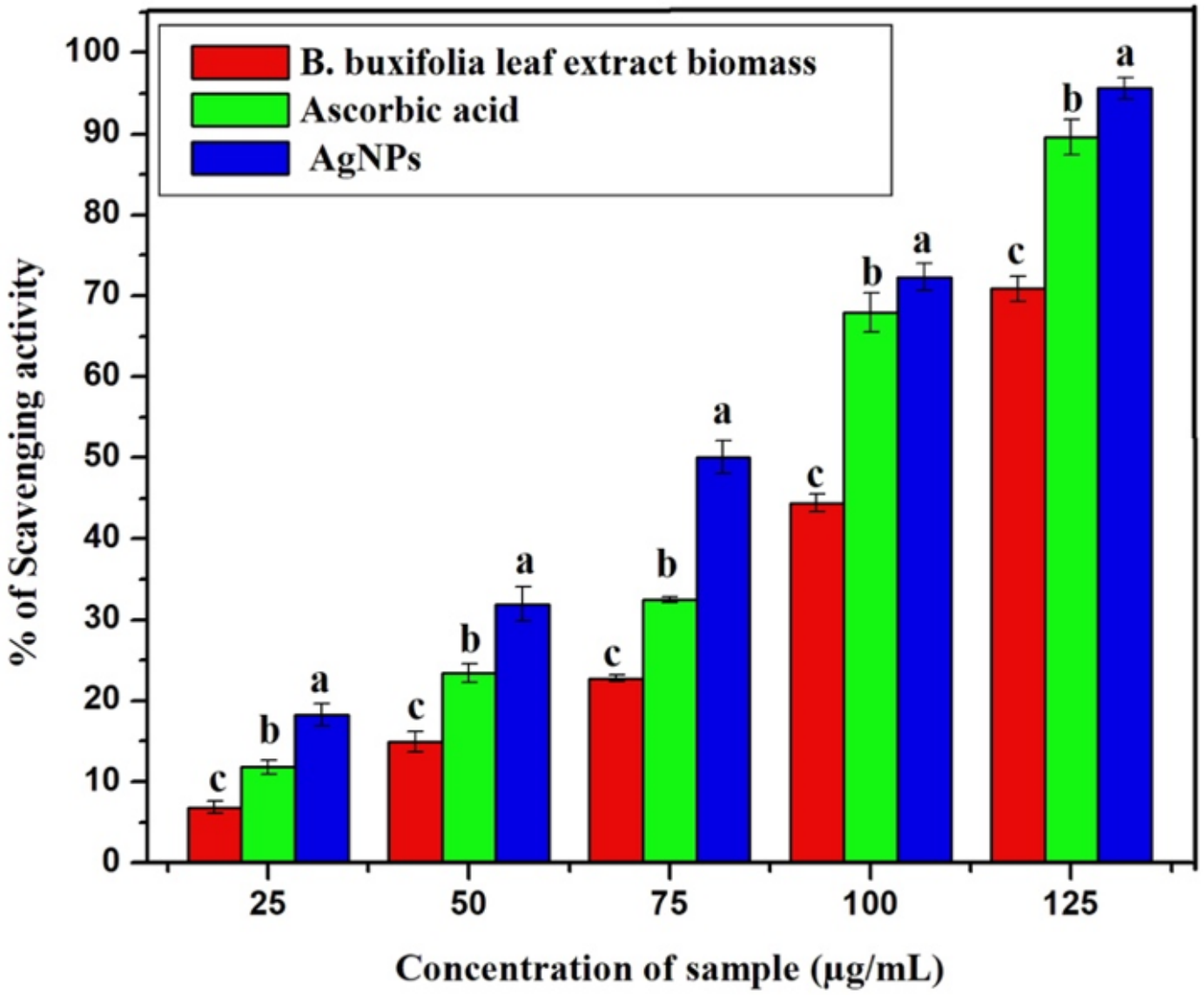

Figure 2

ABTS radical scavenging activity

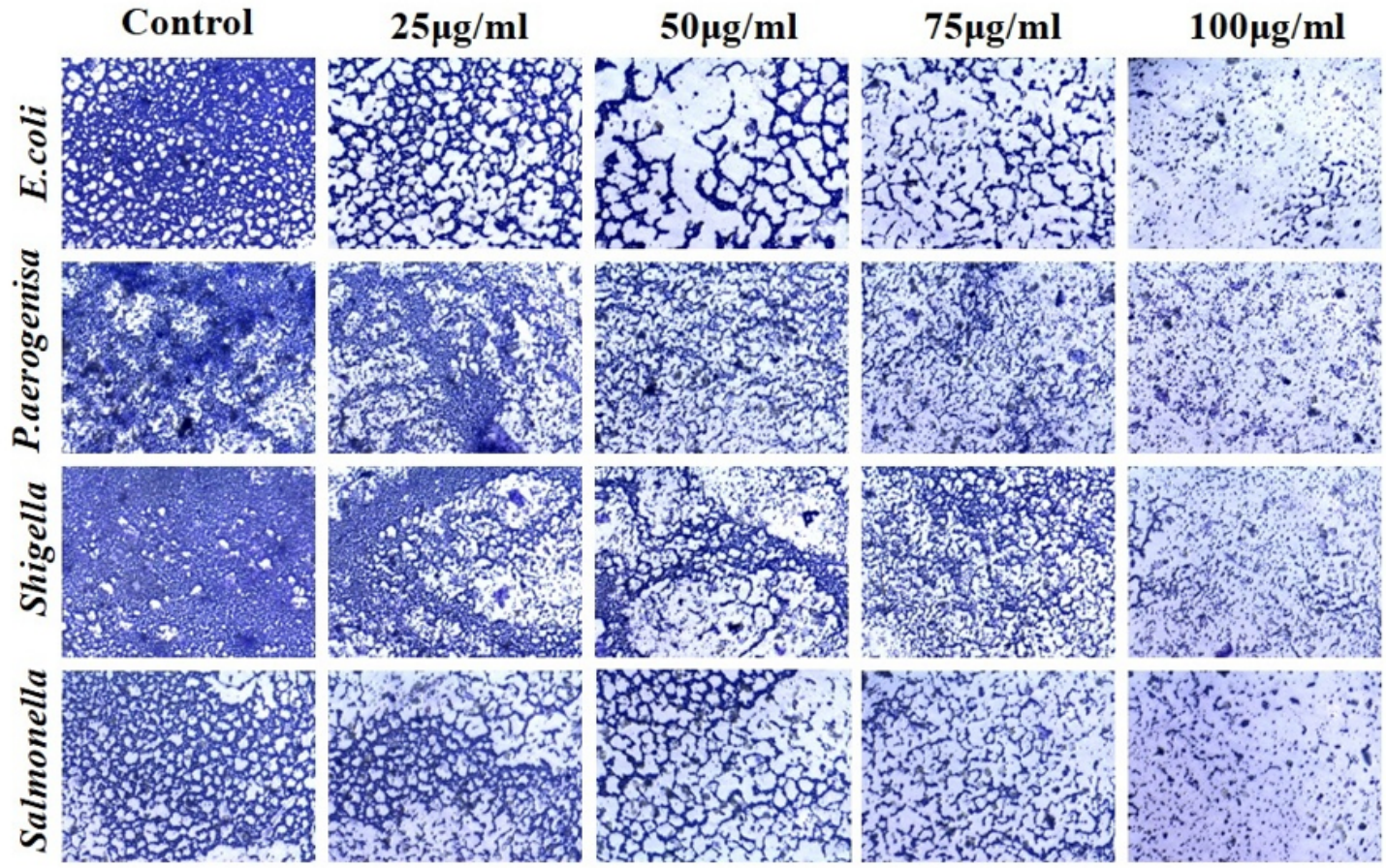

Figure 3

Light Microscopic observation (x40) of bacterial adhesion phases on the glass surfaces with different concentration (control, 25 µg/ml, 50 µg/ml, 75 µg/ml, 100 µg/ml) of synthesized AgNPs against control which is indicative of glass surface with uniformly distributed cells stained with crystal violet.

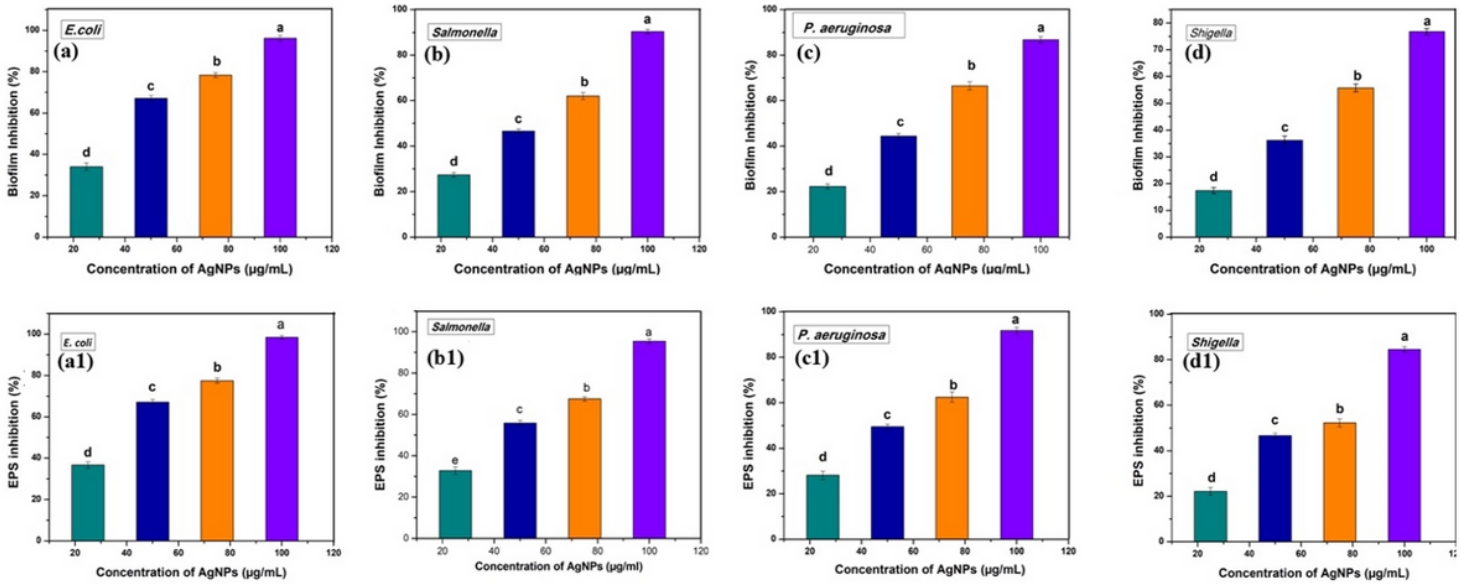

Figure 4

Biofilm quantification using Spectrophotometer assay (a) Anti biofilm activity of synthesized AgNPs against E. coli and P. aeruginosa, S. enterica, Shigella spp with different concentration (control, 25 µg/ml, 50 µg/ml, 75 µg/ml, 100 µg/ml, which are summarized a, b, c, d; EPS reduction activity of AgNPs against same bacteria which are displayed in a1, b1,c1, d1. The data represent the mean values of three independent experiments and are presented as mean ± SD of the absorbance. Mean values within the column followed by the same ANOVA letter in superscript are significantly different at P < 0.05 level.

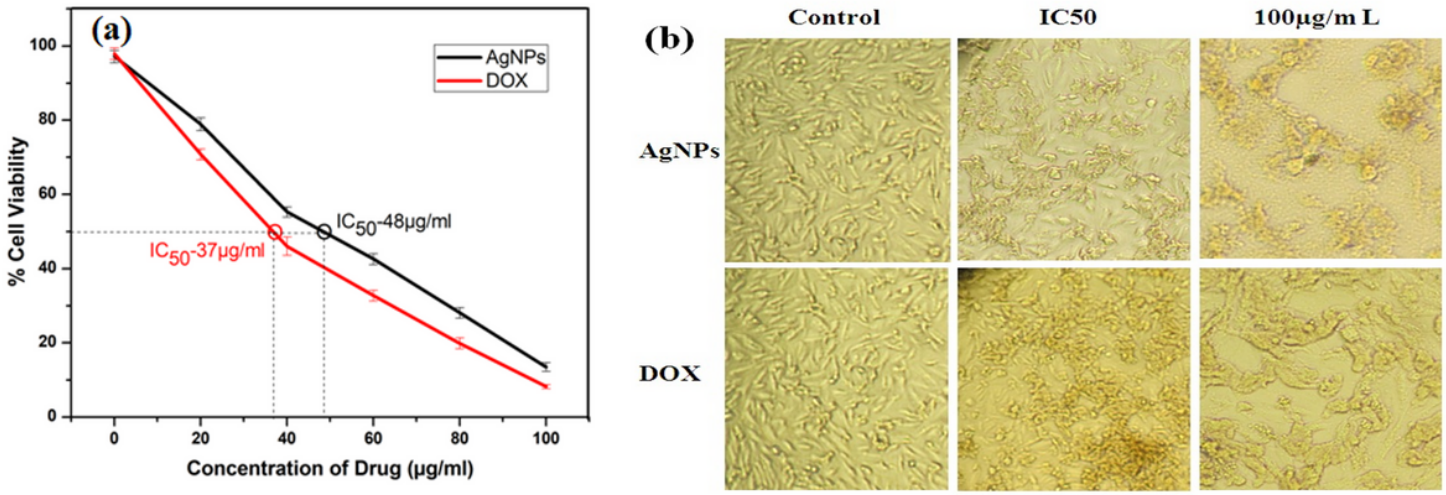

Figure 5

Effect of AgNPs on cell viability of (a) MCF-7 Cells were treated with experimental reagent for 48 h after which viability was measured using the MTT assay. Results are presented as the mean ± S.E.M of experiments conducted at least in triplicate, (b) Light Microscopic observation of MCF-7 Cells treated with IC50,100 g/mL concentration of AgNPs and DOX.

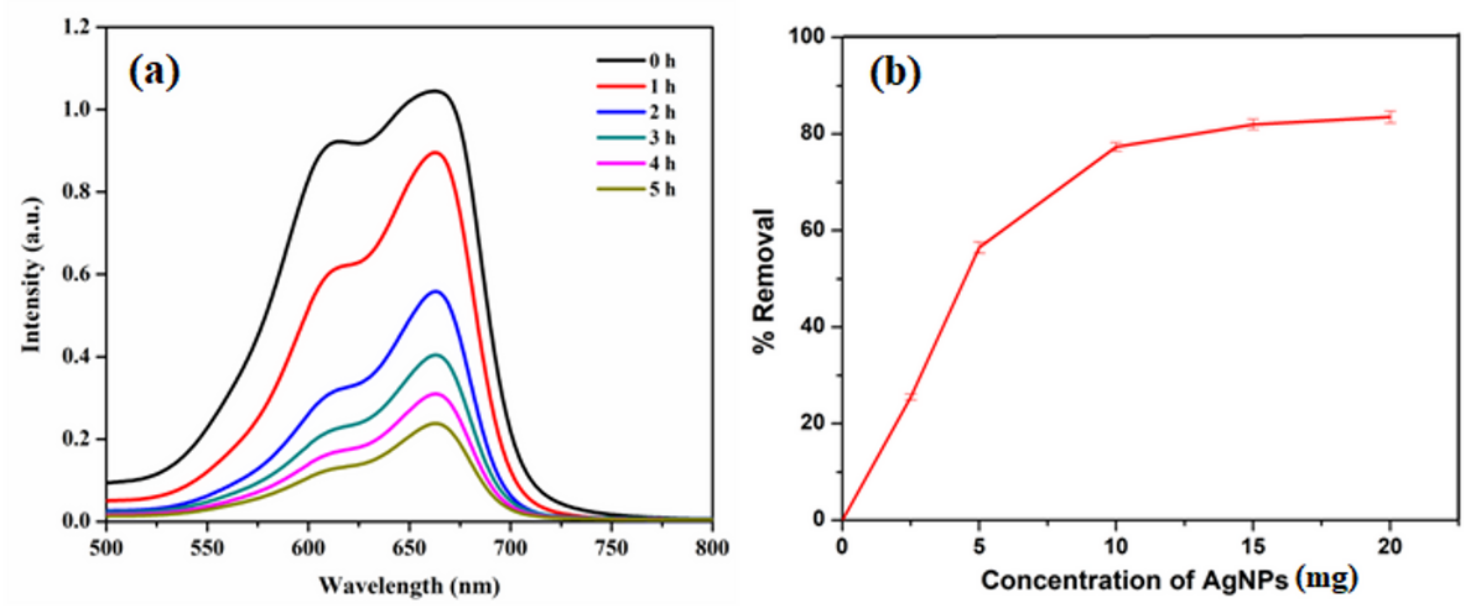

Figure 6

UV-Vis spectra for the photocatalytic reduction of methylene blue (a) Photo-degradation efficiencies of methylene blue as a function of irradiation time by AgNPs, (b) Effect of catalyst concentration (5-20 mg).